

# Improved Performance of 1.55 $\mu\text{m}$ InGaAsP/InP Superluminescent Diodes by Tapered Stripe Structure

Young-Kyu Choi<sup>†</sup>

**Abstract** - We proposed a structure for a 1.55  $\mu\text{m}$  strained separate confinement heterostructure (SCH) multi- quantum well (MQW) superluminescent diode (SLD), having a tapered active region. SLD was fabricated through a two-step procedure: the first step being metal organic chemical vapor deposition (MOCVD) and the second-step being liquid phase epitaxy (LPE). We used a 15° laterally tilted stripe and window region to suppress the lasing action of the SLD. The performance of the SLD showed output power of 11 mW with no lasing under 200 mA pulse driving. The full-width at half-maximum was 42 nm at 200 mA, 25°C.

**Keywords:** effective reflectivity, heterostructure, light source, superluminescent diode

## 1. Introduction

Among the many light sources for fiber optic systems, superluminescent diodes (SLDs) are highly interesting devices [1]. Therefore, SLDs have been broadly utilized as the optimum light sources for application in optical measurement systems such as fiber optic gyroscopes, optical time domain reflectometers, wavelength division multiplexing systems, and short or medium distance optical communication systems. [2-5].

According to the previous reports, SLDs have been divided into two types: SLD-based GaAs operating at approximately 0.8  $\mu\text{m}$ , and SLD-based InPs operating at approximately 1.3 or 1.55  $\mu\text{m}$ . The former yields stable high-output power quite easily. The latter has been developed as the light source for low-loss optical measurement systems, and for high-sensitivity fiber-optic gyro systems.

Generally, the SLD requirements are high-output power, efficient coupling into single-mode fibers, and suppression of lasing due to Fabry-Perot under high-output power operation. In order to suppress the Fabry-Perot mode, several methods have been proposed: placing anti-reflection (AR) coating at one or two facets, tilting the stripe in respect to the facets, bending the stripe near the output facet or rear facet, dry etching the rear facet at an angle to the stripe, placing a window structure near the rear facet, and employing an unpumped absorbing region near the rear facet. However there are limitations to reducing the reflectivity by only using AR coating. Thus, in order to obtain a broad spectral width, one or two of the above-

mentioned methods are often used together with AR coating.

In this paper, we have reported on the characteristics of a 1.55  $\mu\text{m}$  strained SCH-MQW SLD, which has a window region laterally tilted taper active layer. The SLD device is fabricated by using, first, MOCVD and then, second, LPE to form the planar buried hetero structure (PBH) to confirm the transverse current. All the devices are fabricated without AR coating to reduce reflectivity at both facets.

## 2. Fabrication of the Devices

The schematic structure of the SLD is shown in Fig. 1. To attain extremely low reflectivity, we introduced a window region on the front and rear side of the SLD. The light beam that travels backward is emitted from the edge of the active layer and diverges in the window region. Then, the beam is reflected at both facets by only a few percents, a fraction of which couples into the active layer. Thus, this window structure provides a remarkable level of reflectivity reduction at the interface between the active region and the window region. The effective reflectivity can be reduced even further by increasing the length of the window region [6]. The reduction of the reflectivity is the key feature of this structure that makes it possible to easily obtain SLD operation without lasing operation. As well, the SLD is laterally tilted by 15°, which further reduces the reflectivity between the active region and the window region [7].

Generally, if we consider the coupling between the device and a single mode fiber, the tilted angle of the SLDs is proper to 7°. However, the previous device that is laterally tilted by 7° was happened to lasing action. By

<sup>†</sup> Corresponding Author: Division of Photonics, Faculty of Engineering, Silla University, Korea. (ykchoi@silla.ac.kr)

Received October 3, 2004 ; Accepted November 4, 2004

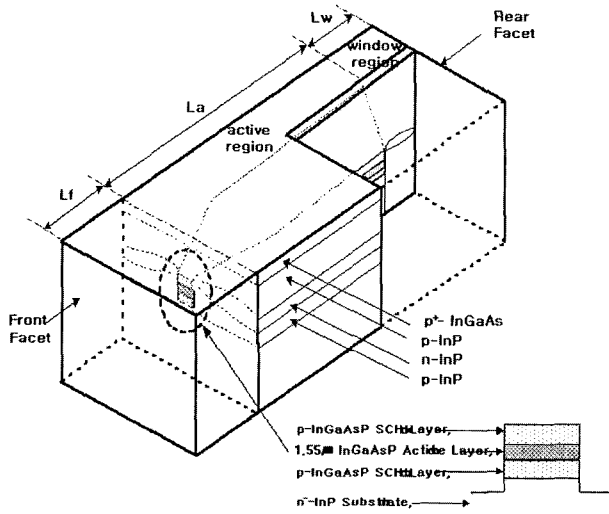


**Fig. 1** Schematic structure of 1.55  $\mu\text{m}$  InGaAsP/ InP MQW-PBH-SCH SLD with a window region.

means of the theoretical reflectivity calculation, we know that 13-18° is appropriate for the tilted angle in the case that the stripe width is 1.5-2  $\mu\text{m}$ . Based on these experiments and calculations, we designed the stripe with the tilted angle of 15°. Also, we use the tapered active layer for the high power operation of the SLD. The total length of the SLD cavity is 1.3 mm. The front window regions and the window regions have the lengths of 200  $\mu\text{m}$ , 300  $\mu\text{m}$ , 600  $\mu\text{m}$ , and 200  $\mu\text{m}$ , respectively.

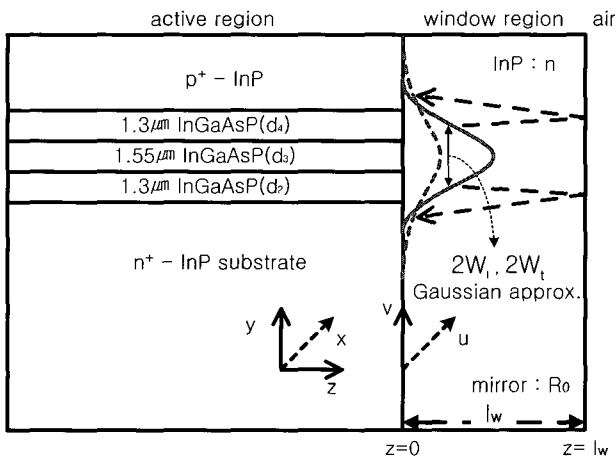


**Fig. 2** Reflection in the window region. The solid line shows the guided field profile in the waveguide assumed to be Gaussian, and the broken line shows the reflected field profile. A small amount of the reflected field is coupled into the waveguide again.

Next, based on the above mentioned structure we have calculated the effective reflectivity as a function of the length of the window region, tilted angle, and active layer

width theoretically. Fig. 2 indicates the reflection in the window region [6]. The guided field in the waveguide (a solid line) is emitted into the window region of the InP.

The refractive index and length of the window region are  $n$  and  $l_w$ , respectively, and  $W_1$  and  $W_2$  are the respective spot sizes in the  $x$  and  $y$  directions. For simplicity, we suppose that the guided field profile is Gaussian in the rectangular waveguide. We have calculated the effective reflectivity  $R_{\text{eff}}$  in the window structure. The effective reflectivity [6] of the window for the rectangular waveguide is provided as

$$R_{\text{eff}}(l_w) = R_0 \frac{\sqrt{1 + \frac{4l_w^2}{k^2 w_1^4}}}{\sqrt{\left(1 + \frac{4l_w^2}{k^2 w_1^4}\right)^2 + \frac{4l_w^2}{k^2 w_1^4}}} \frac{\sqrt{1 + \frac{4l_w^2}{k^2 w_2^4}}}{\sqrt{\left(1 + \frac{4l_w^2}{k^2 w_2^4}\right)^2 + \frac{4l_w^2}{k^2 w_2^4}}} \quad (1)$$

where,  $R_0$  is the reflectivity of a cleaved mirror, and the value of the uncoated mirror is about 0.3. The transverse and lateral direction spot size was calculated with Gaussian approximation. The calculated results of  $R_{\text{eff}}$  are shown in Fig. 3 as a function of the window length and the degree of facet coating. The thickness of the active layer and separate confinement layers were 0.2  $\mu\text{m}$  and 0.08  $\mu\text{m}$ , respectively. We know that the effective reflectivity is reduced as the window region length is increased and the active layer

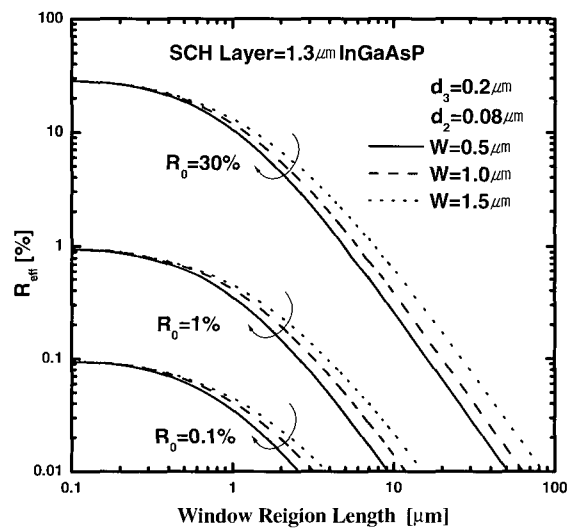


**Fig. 3** Effective reflectivity of the window structure  $R_{\text{eff}}$  as a function of the window length, active layer width, and  $R_0$ .

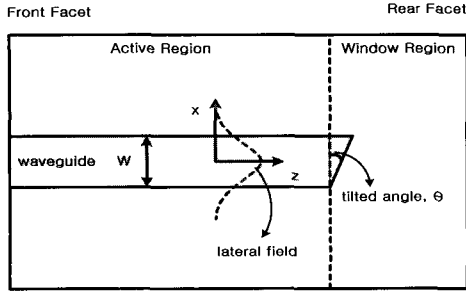


Fig. 4 Slab waveguide structure with laterally tilted angle.

width is decreased. For example, in order to cause the reduction level to be below the reflectivity of  $10^{-4}$ , the window region length must be over  $80 \mu\text{m}$  when the active layer width is about  $1.5 \mu\text{m}$ . Another method to reduce the reflectivity is tilted interfaced between the waveguide of the active region and the window region. Therefore, the reflectivity is effectively reduced at the interface. The end of the waveguide is contacted in the window region as a tilted degree of  $\theta$  as is shown in Fig. 4. For a perfect mirror, to find the reflection coefficient of the guided mode that turns back on itself is the equivalent of computing the tilt loss for a slab waveguide of tilt angle  $2\theta$ . For a mirror

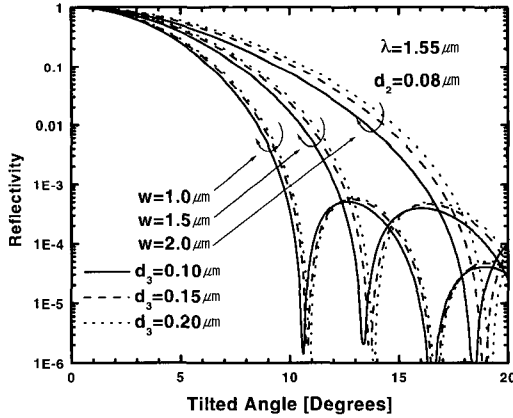


Fig. 5 Fundamental TE mode reflectivity with tilted angle, active layer thickness, and width.

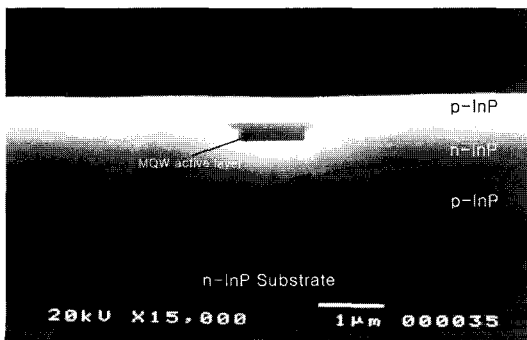


Fig. 6 SEM cross sectional photograph of the grown planar buried heterostructure

of finite reflectivity, the tilt loss must be multiplied by the Fresnel reflection loss corresponding to the tilted mirror. Therefore, the power reflection coefficient of the waveguide is given by

$$R_g = R_f(\theta) |c^2| \quad (2)$$

where,  $R_f(\theta)$  is the fresnel reflection coefficient of a plane wave that is reflected from the tilted interface between the window region and the active region.  $C$  is the amplitude transmission coefficient. We calculated the reflectivity with tilted angle by using equation (2), which was plotted in Fig. 5. Fig. 6 shows the SEM cross sectional photograph of the grown planar buried hetero structure. As further depicted in Fig. 6, the p-type and n-type InP current blocking layer were grown to reduce leakage current. The SLD device was fabricated by using, first, MOCVD and second, LPE. In the first growth step using MOCVD, an n-InP buffer layer, a  $1.55 \mu\text{m}$  strained SCH MQW, and a p-InP layer were grown in sequence. The strained MQW consists of seven pairs of a 0.7% compressively strained InGaAsP ( $\lambda_g=1.55 \mu\text{m}$ ) well and a 0.35% tensile-strained InGaAsP ( $\lambda_g=1.24 \mu\text{m}$ ) barrier, surrounded by n- and p-InGaAsP ( $\lambda_g=1.2 \mu\text{m}$ - $1.1 \mu\text{m}$ ) separate confinement layers. Trimethyl indium (TMIn) and triethyl gallium (TEGa), together with phosphines ( $\text{PH}_3$ ) and arsine ( $\text{AsH}_3$ ), were used as precursors.

The designed SLD mask pattern for the active region was aligned along the [110] direction of the first growth wafer using the photolithography process. For the formation of p-n-p current blocking, a mesa structure is formed by the two-step wet etching process [8].

After the formation of the mesa structure, the second growth step for current blocking is accomplished by LPE. The main procedure for LPE is as follows: source materials (In, InP) with high purity (>99.999%) are chemically rinsed and then weighed.

Te and Zn were used as n- and p-type dopants. It is necessary to mix the source materials before LPE growth in a baking process. All the weighed materials for growth are mixed completely at  $630 \text{ }^\circ\text{C}$  in the atmosphere of high-purified  $\text{H}_2$  for three hours to prepare the uniformly distributed melts. To avoid pollution between growths due to the evaporation of volatile ingredients, all the melts are prepared separately.

After the preparation of all the melts, InP substrate is put into the graphite boat for the epitaxial growth process. The melting temperature for growth melts is  $610 \text{ }^\circ\text{C}$ , and the melting process will keep for a period of 30min, after which process, the temperature of the growth system is lowered with a cooling rate of  $1 \text{ }^\circ\text{C}/\text{min}$ . To avoid thermal

damage of the substrate, the growth of the p-n-p blocking layer begins at the 600 °C, and three layers of p-InP ( $N_d = 7 \times 10^{17} \text{ cm}^{-3}$ ), n-InP ( $N_a = 7 \times 10^{18} \text{ cm}^{-3}$ ), and p-InP ( $N_d = 7 \times 10^{17} \text{ cm}^{-3}$ ) are grown by turns.

The last, a p-InP ( $N_d = 1 \times 10^{18} \text{ cm}^{-3}$ ) clad layer and a p-GaInAs ( $N_d = 2 \times 10^{19} \text{ cm}^{-3}$ ) cap layer are also grown by LPE following removal of the  $\text{SiN}_x$  mask using the same method mentioned above. The growth temperature of the p-InP clad layer and p-InGaAs ohmic layer is 600 °C, and 596 °C, respectively. Ti/Pt/Au and Cr/Au electrodes are formed on the top and the bottom of the wafer as p-type and n-type ohmic contacts, respectively.

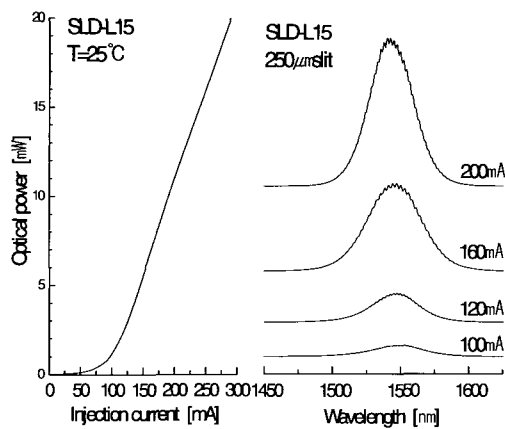


**Fig. 7** Optical output power vs. current characteristic, and emission spectrum characteristics, of a 1.55  $\mu\text{m}$  SLD-L15.

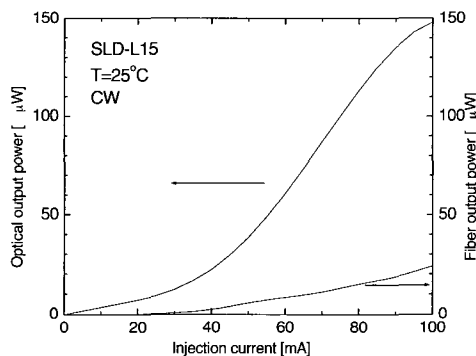


**Fig. 8** Optical output power and fiber coupled power versus driving current. SLD was coupled into an inclined single mode fiber.

### 3. Discussions

Fig. 7 presents the optical output power versus current characteristic, and the emission spectrum versus driving current characteristics, of 1.55  $\mu\text{m}$  SLD-L15 at 25 °C. The

emission wavelength is centered about 1.55  $\mu\text{m}$  with a spectrum width of 42 nm and the device has less than 5% spectral modulation  $(I_{\text{max}} - I_{\text{min}})/(I_{\text{max}} + I_{\text{min}})$  at a power level of 200 mA. The fundamental transverse mode operation was confirmed up to 200 mA. In consideration of the application for an optical module, we measured the dc characteristics. Fig. 8 displays the optical output power characteristics versus driving current at an ambient temperature of 25 °C under dc operation. 150  $\mu\text{W}$  is emitted from the facet at 100 mA. In Fig. 8, we display the fiber-coupled power characteristics. We coupled the SLD into an inclined single-mode fiber. The power of about 24  $\mu\text{W}$  is coupled into the single mode fiber at a driving current of 100 mA. We then achieve coupling efficiency of 16 %.

### 4. Conclusion

In order to suppress lasing oscillation, we proposed laterally-tilted MQW-PBH-SCH SLDs with a window region and tapered active layer. The devices were fabricated by using MOCVD and LPE equipment. We calculated the effective reflectivity of the window structure as a function of the window length. Also, we calculated the fundamental TE mode reflectivity with tilted angle, active layer thickness and width. The output power, the spectral width, and spectral modulation of SLD-L15 were 11 mW, 42 nm, and 5%, respectively, at 200 mA under pulse operation and 25 °C. We achieved the coupled power of 24  $\mu\text{W}$  and coupling efficiency of 16% with an inclined single mode fiber at 100mA under dc operation and 25 °C.

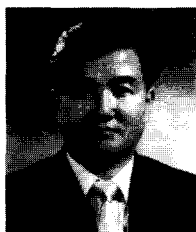
### Acknowledgements

The author would like to thank Dr. Kim Jeong-Ho of the Korea Maritime University for technical assistance in wafer growth service, device fabrication and also for participation in highly useful discussions. In addition, the author would like to thank Professor Hong Tchang-Hee of the Korea Maritime University for his beneficial influence.

### References

- [1] Toru Takayama, Osamu Imafuji, Yasuyuki Kouchi, Masaaki Yuri, Member, IEEE, Akio Yoshikawa, and Kunio Itoh, IEEE J. Quantum Electron., 32, 1981 (1996).
- [2] W. K. BURNS, R. P. MOELLER, And A. DANDRIDGE, IEEE Photonics Tech. Lett., 2, 606

- (1990).
- [3] Takeshi YAMATOYA, Shota MORI, Fumio Koyama and Kenichi IGA, *Jpn. J. Appl. Phys.* 38, 5121 (1999).
  - [4] N. S. K. KWONG, K. Y. LAU, AND N. BAR-CHAIM, *IEEE J. Quantum Electron.*, 25, 696 (1989).
  - [5] S. S. WAGNER, T. E. CHAPURAN, *Electron. Lett.*, 26, 696 (1990).
  - [6] Katsuyuki Utaka, Shigeyuki Akiba, AND Yuichi Matsushima, *IEEE J. Quantum Electron.*, 20, 236 (1984).
  - [7] Dietrich MARCUSE, FELLOW, IEEE, *J. Lightwave Tech.*, 7, 336 (1989).
  - [8] Ho Sung CHO, Dong Hoon JANG, Jung Kee Lee, Kyung Hyun PARK, Jeong Soo KIM, Seung Won LEE, Hong Man KIM and Hyung-Moo PARK, *Jpn. J. Appl. Phys.*, 35, 1751 (1996).



#### **Young-Kyu Choi**

He received his M.S. and Ph.D degrees from Kyoto University, Kyoto, Japan in 1989, and 1992, respectively. From 1993 to 1995, he was a Full-time Lecturer in the Department of Electronics, Fukui University, Fukui, Japan. He is now an Associate

Professor in the Department of Photonics, Silla University, Busan, Korea. His research interests include the ultra-high-speed optical communication system, optical modulator and demodulator, optical waveguide analysis, optical sensors, microwave photonics, and near-field lightwave technology. He is presently a member of the KIEE, IEICE, JJAP, OSA, and IEEE.

Tel: +82-51-309-5622, Fax: +82-51-309-5622